Journal of Alloys and Compounds 509 (2011) 5587–5590

Contents lists available at ScienceDirect

Journal of Alloys and Compounds

journal homepage: www.elsevier.com/locate/jallcom

Effect of Ta seed layer on crystalline structure and magnetic properties in an exchange-biased Co/IrMn system

Yuan-Tsung Chen[a,*], Y.C. Lin[a], S.U. Jen[b], Jiun-Yi Tseng[b], Y.D. Yao[c]

[a] Department of Materials Science and Engineering, I-Shou University, Kaohsiung 840, Taiwan, ROC
[b] Institute of Physics, Academia Sinica, Taipei 11529, Taiwan, ROC
[c] Graduate Institute of Applied Science and Engineering, Fu Jen Catholic University, Taipei 242, Taiwan, ROC

ARTICLE INFO

Article history:
Received 14 October 2010
Received in revised form 11 January 2011
Accepted 21 January 2011
Available online 23 February 2011

Keywords:
Seed layer effect
IrMn (1 1 1) texture
Exchange-biasing field (H_{ex})
Coercivity (H_c)

ABSTRACT

Ta-seeded and un-seeded layers of a top-configuration Co/IrMn system were deposited onto glass substrate by DC sputtering. Three sets of deposition conditions for Co(50 Å)/IrMn(t_{IrMn} Å) and Co(t_{Co} Å)/IrMn(90 Å), where t_{IrMn} = 15, 30, 60, 90, 110, and 150 Å, and t_{Co} = 15, 25, 50, 75, 100, 125, and 150 Å, were: condition (a) substrate temperature (T_s) was kept at room temperature (RT). Condition (b) T_s set to RT, with in-plane magnetic field, H = 500 Oe. In condition (c), condition (b) was followed by post-deposition annealing in the magnetic field at T_A = 250 °C for 1 h, then field cooled to RT. X-ray diffraction (XRD) patterns and grazing incidence scans revealed maximum IrMn (1 1 1) texture to occur for post-deposition annealed Ta seed layer samples. The IrMn (1 1 1) texture-effect significantly influences magnetic properties, including exchange-biasing field (H_{ex}), interfacial energy (J_k), and coercivity (H_c). The Ta seed layer also significantly influences magnetic properties. Adding a Ta seed layer to the Co/IrMn system increases H_{ex}, because of the IrMn (1 1 1) texture. For Ta-seeded Co/IrMn under condition (c), H_{ex} tended to saturate for $t_{IrMn} \geq 90$ Å. Under conditions (a) and (b), H_{ex} decreased with increasing t_{IrMn} for $t_{IrMn} \geq 90$ Å. H_{ex} values for all un-seeded Co/IrMn systems increased with t_{IrMn}. J_k versus t_{IrMn} plot is proportional only to H_{ex} in the Ta-seeded and un-seeded layers of a top-configuration Co/IrMn system, due to the interfacial energy formula, t_{Co} is fixed, and saturation magnetization (M_s) of the Co layer is constant. Results for the Ta-seeded system showed a strong relationship between H_c and t_{IrMn}, due to coupling-decoupling interactions between Co spin, and IrMn layers close to the Co/IrMn interface. The H_{ex} versus t_{Co} result shows that the H_{ex} is proportional to ($1/t_{Co}$). The H_{ex} values with the Ta seed layer are almost slightly larger than those without a Ta seed-layer. The dependence of J_k on t_{Co} is similar to the trend in M_s on t_{Co}, J_k tends to saturate slowly as t_{Co} increases. Surface pinning occurred in all systems, revealing an inverse relation between H_c and t_{Co}. Removing the Ta seed-layer weakens IrMn (1 1 1) texturing, reducing H_{ex}. The maximum observed H_{ex} and J_k values were 205 Oe and 0.11 erg/cm^2, respectively.

1. Introduction

Magnetoresistance random access memory (MRAM) and recording-head applications could exploit ferromagnetic (FM)/antiferromagnetic (AFM) interface exchange-coupling interactions, which cause a unidirectional shift in the magnetic hysteresis loop exchange-bias [1–5]. Numerous factors, including the IrMn (1 1 1) texture, the AFM layer ordered and disordered phases, post-annealing scheme, and the seed layer effect [6–9], can influence FM/AFM magnetic properties. Researchers attributed the larger exchange-biasing field (H_{ex}) to a stronger IrMn (1 1 1) texture, where the seed layer deposition-candidate is crucial [10–12]. There is a strong relationship between H_{ex} performance and IrMn layer characteristics, including (1 1 1) texture, anisotropy constant (K_{AF}), grain size distribution, and AFM grain thermal-stability [10–14]. The seed layer is probably the dominant factor affecting microstructural orientation, reduction in current shunting for grain magnetoresistance (GMR), and the tunneling magnetoresistance (TMR) effect [13,14]. Moreover, removing the Ta seed layer from the Co/IrMn system results in poor IrMn (1 1 1) texture, and reduces H_{ex} values. Thus, there is a close relationship between the seed layer effect, and magnetic performance variables such as exchange-biasing system H_{ex} and coercivity (H_c).

We deposited a top-configuration Co/IrMn system onto glass substrate under three different deposition conditions, described in the following experimental procedure section. This investigation

* Corresponding author at: Department of Materials Science and Engineering, I-Shou University, Kaohsiung Taiwan 840, ROC No. 1, Sec. 1, Syuecheng Rd., Dashu Township, Kaohsiung County 840, Taiwan. Tel.: +886 765 777 11; fax: +886 765 784 44.
E-mail address: ytchen@isu.edu.tw (Y.-T. Chen).

0925-8388/$ – see front matter © 2011 Elsevier B.V. All rights reserved.
doi:10.1016/j.jallcom.2011.01.218

focuses on the relationship between IrMn (1 1 1) texture and the materials magnetic properties.

2. Experimental procedures

The top configuration Co/IrMn system was fabricated on glass substrate by DC magnetron sputtering. We considered two cases: (A) devices without a Ta seed layer and (B) devices with a Ta seed layer. The Ta-seeded and un-seeded multilayer deposition sequences were, respectively: (1) Glass/Ta(30 Å)/Co(50 Å)/IrMn(t_{IrMn} Å)/Ta(100 Å) and Glass/Co(50 Å)/IrMn(t_{IrMn} Å)/Ta(100 Å), where t_{IrMn} = 15, 30, 60, 90, 110, and 150 Å. (2) Glass/Ta(30 Å)/Co(t_{Co} Å)/IrMn(90 Å)/Ta(100 Å) and Glass/Co(t_{Co} Å)/IrMn(90 Å)/Ta(100 Å), where t_{Co} = 15, 25, 50, 75, 100, 125, and 150 Å. The top Ta(100 Å) layer served as a protective layer to prevent oxidation of IrMn. For each system, we applied three different sets of deposition conditions: (a) the substrate temperature (T_s) was maintained at room temperature (RT) in the absence of any magnetic field. (b) T_s was RT, with an in-plane magnetic field, H = 500 Oe, during deposition. (c) Condition (b) was followed by post-deposition annealing in the field at 250 °C (T_A) for 1 h, then cooled to RT in the magnetic field. The use of Ta as a seed layer produces a strong (1 1 1) texture in the Co and IrMn layers [15]. The composition of the IrMn alloy target was 20 at.% Ir and 80 at.% Mn. Typical base chamber pressure was 2×10^{-7} Torr, and the argon gas working pressure was 5×10^{-3} Torr.

The degree of $Ir_{20}Mn_{80}$ (1 1 1) layer texturing was characterized by X-ray diffraction (XRD) and grazing incidence (GIXD) scans at a grazing angle of 1°, using Cu $K\alpha_1$ radiation. The LakeShore Model 7300 vibrating sample magnetometer (VSM) provided the exchange-biased magnetic hysteresis loop for training effect removal.

3. Results and discussion

First, we emphasized the two cases (A and B) again, respectively. The case A means that the Co/IrMn system is no Ta seed layer structure. In contrast, the case B means that the Co/IrMn system has the Ta seed layer structure. Fig. 1(a) shows the Co(50 Å)/IrMn(110 Å) XRD patterns, for each case (A and B) in the same post-annealing process. Fig. 1(a) compares the X-ray results for the two cases. The Co/IrMn system with a Ta seed layer (case B), has a crystalline body-centered cubic (BCC) structure, producing β-Ta (2 0 0) and Ta (1 1 0) peaks. Moreover, the diffraction intensities of Co (1 1 1) and IrMn (1 1 1) planes in case B were much stronger than those in case A, indicating that the inclusion of a Ta seed layer, results in the Co and IrMn layers having more crystalline character. Fig. 1(b) shows the corresponding grazing angle scans to Fig. 1(a). The spectrum shows that the annealed Ta seed-layer sample produces strong IrMn (1 1 1) and Co (1 1 1) in-plane diffraction-peaks. By contrast, in the absence of a Ta seed layer in the annealed sample, only weak IrMn (1 1 1) and Co (1 1 1) peaks appear. Fig. 1(c) shows that IrMn (1 1 1) X-ray peak intensity is dependent on the thickness (t_{IrMn}) of IrMn in each case. Post-annealing treatment of case B (with a Ta seed layer) samples produces the strongest IrMn (1 1 1) texture, while the IrMn (1 1 1) peaks of the remaining samples are weak and less intense. Accordingly, adding a Ta seed layer, without post-annealing treatment, does not necessarily strengthen IrMn texturing.

Fig. 2(a) is a plot of the exchange field (H_{ex}), as a function of IrMn thickness (t_{IrMn}). This plot shows that the Ta seed layer significantly influences magnetic properties. Adding a Ta seed layer to the Co/IrMn system increases H_{ex} due to the IrMn (1 1 1) plane, that provides the largest possible spin density at Co/IrMn interfaces [16]. Therefore, H_{ex} in case A (without a Ta seed layer) is generally lower than that in case B (with a Ta seed layer). In both cases A and B, H_{ex} increases with t_{IrMn}, from 15 Å to 60 Å. H_{ex}, for Ta-seeded Co/IrMn under condition (c), tends to saturate at $t_{IrMn} \geq 90$ Å, while for Ta-seeded Co/IrMn under conditions (a) and (b), H_{ex} tends to decline as t_{IrMn} increases over this range, because of the IrMn texture defect [11]. By contrast, the H_{ex} value for all the un-seeded Co/IrMn systems tends to increase slightly with t_{IrMn}. Fig. 2(b) plots interfacial energy (J_k) versus t_{IrMn}, using a well-established formula,

$$J_k = H_{ex} M_s t_{Co}, \quad (1)$$

where M_s is the saturation magnetization of the Co layer and t_{Co} is the Co layer thickness. Since t_{Co} is fixed 50 Å in both cases A and B,

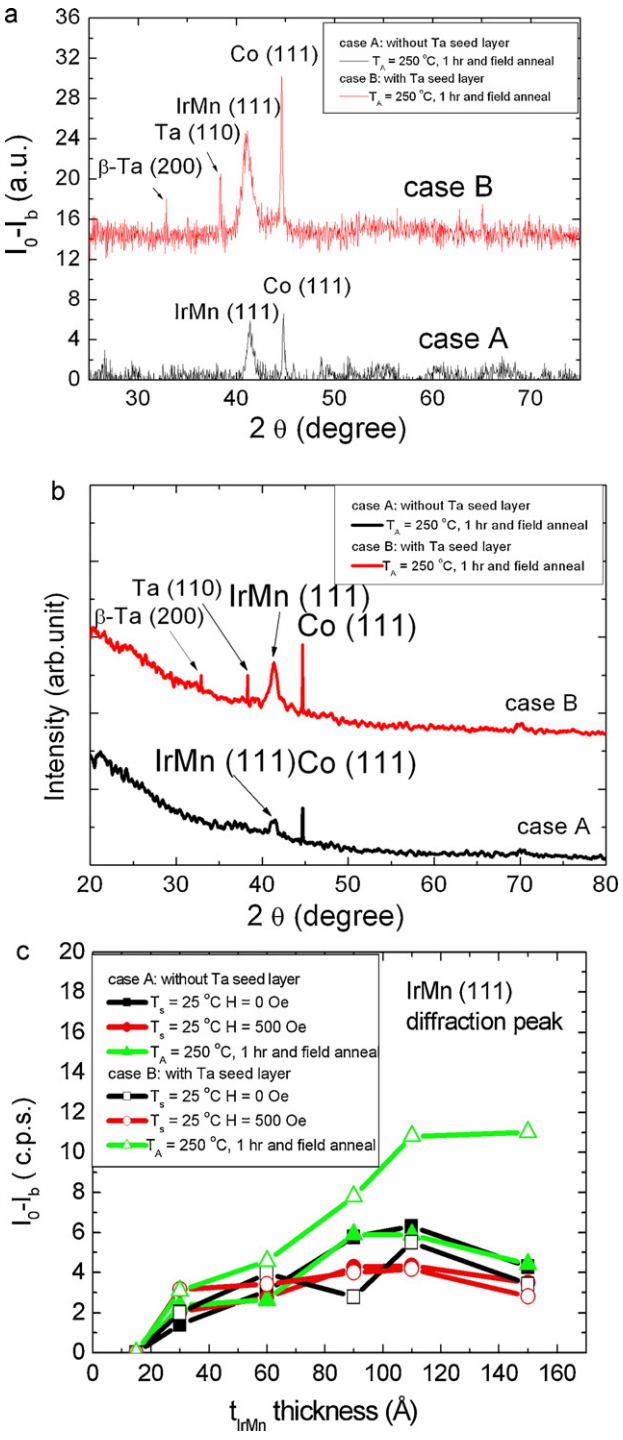

Fig. 1. (a) X-ray diffraction plots in cases A and B. I_o is the absolute intensity and I_b is the background intensity. (b) Grazing angle result for post-annealing samples with cases A and B. (c) Degree of IrMn (1 1 1) texture, as determined from the X-ray diffraction results, plotted as function of t_{IrMn} for cases A and B. I_o is the intensity of the IrMn (1 1 1) line and I_b is the background intensity.

and M_s is constant, then, J_k is proportional only to H_{ex}, as shown in Fig. 2(b). According to the above results of the XRD analysis and exchange-biasing magnetic hysteresis loop measurement, not only the density of spins at the Co/IrMn interface, but also J_k increases due to the presence of Ta seed layer, and to the field annealing treatment. This indicates that the effects of both Ta seed layer, and field annealing treatment, on exchange-coupling interactions at the Co/IrMn interface are significant and effective. In view of literature reports regarding exchange-biasing, higher J_k can over-

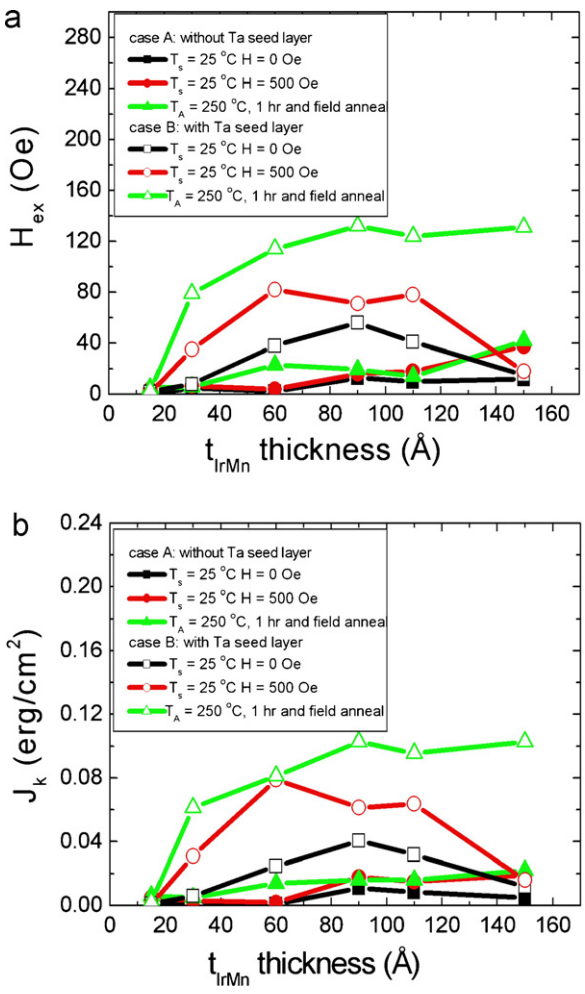

Fig. 2. (a) Dependence of the exchange-biasing field (H_{ex}) on IrMn thickness (t_{IrMn}) in cases A and B, and under conditions (a) to (c). (b) Dependence of interfacial energy (J_k) on IrMn thickness (t_{IrMn}) in cases A and B.

come the spin rotation barrier, so making spin rotation more facile [17,18].

Fig. 3 plots H_c versus t_{IrMn} in the two cases A (without a Ta seed layer) and B (with a Ta seed layer). In general, H_c increases as t_{IrMn} increases from 15 Å to 30 Å and then falls as t_{IrMn} increases further, because of the spin coupling and decoupling interaction that

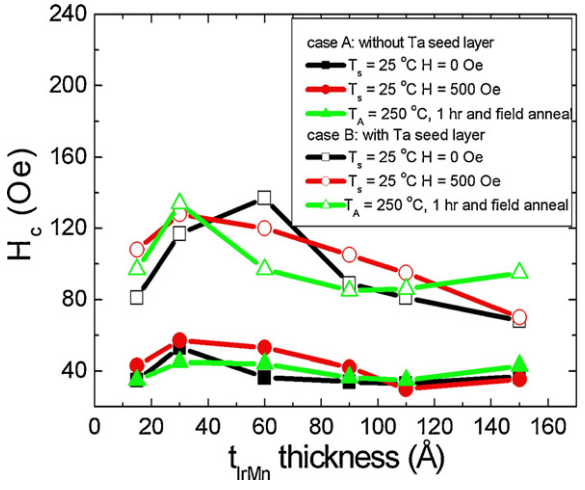

Fig. 3. Coercivity (H_c) versus IrMn thickness (t_{IrMn}) in cases A and B.

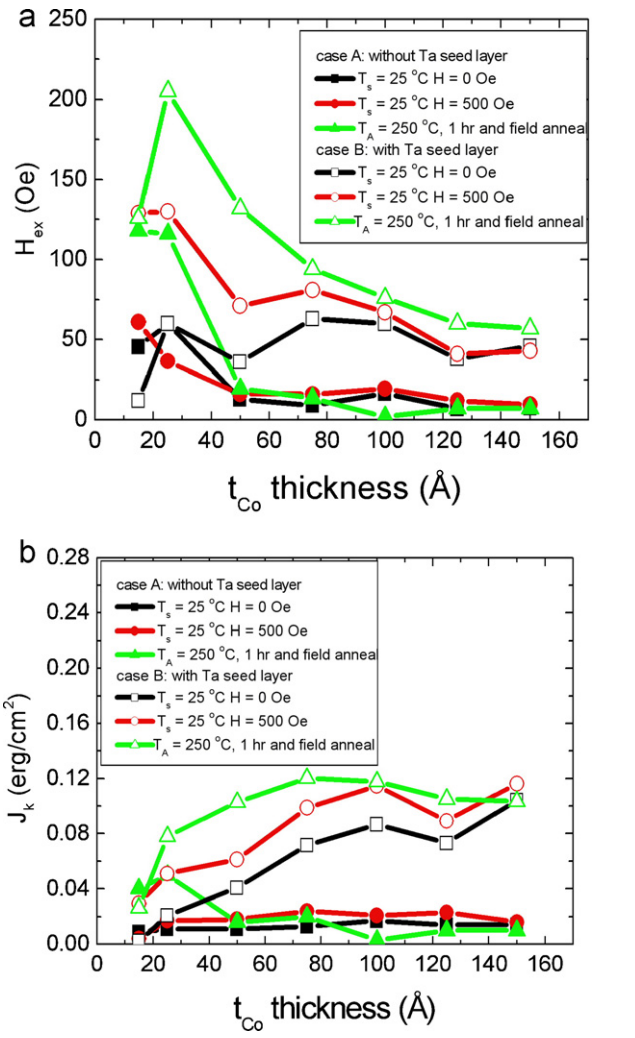

Fig. 4. (a) Dependence of exchange-biasing field (H_{ex}) on Co thickness (t_{Co}) in cases A and B. (b) Dependence of the interfacial energy (J_k) on Co thickness (t_{Co}) in cases A and B.

occur between the Co and IrMn layers at the Co/IrMn interface as t_{IrMn} is slowly increased [19]. Coupling drag occurs at the Co/IrMn interface, causing H_{ex} to increase as t_{IrMn} is increases from 15 Å to 30 Å. The coupling force between Co and nearby IrMn spins at the interface, exceeds the force between neighboring IrMn spins. The external field (H) must induce both the Co spins and IrMn spins, suggesting that H_c increases as t_{IrMn} increases from 15 Å to 30 Å. Furthermore, as t_{IrMn} continues to increase, H_c reaches a maxima, then declines, this is due to decoupling between the interfacial Co spin and the IrMn spin on top. At $t_{IrMn} \geq 30$ Å, when H_{ex} is fully develop, it indicates that the exchange coupling of interfacial Co and IrMn spins becomes weaker. Therefore, IrMn spin at the interface is strongly pinned by the IrMn spins beneath, H_c switches only the Co spin, and no longer switches the neighboring IrMn spin. However, other researchers proposed an alternative explanation for the increase in H_c that occurs with increasing seed layer thickness [20]. Increasing seed layer thickness produces greater roughness, and this results in exchange-decoupled grain and so increases H_c [20]. Moreover, the H_c of an un-seed layer in the Co/IrMn system shows a similar, albeit smaller trend in H_c.

Fig. 4(a) plots the dependence of H_{ex} on the thickness (t_{Co}) of Co in cases A (without a Ta seed layer) and B (with a Ta seed layer). From Eq. (1), H_{ex} (equal to $J_k/(M_s t_{Co})$) is easily derived. Fig. 4(a) shows that, since (J_k/M_s) is constant, then H_{ex} is proportional to ($1/t_{Co}$). Therefore, the H_{ex} values with the Ta seed layer are almost

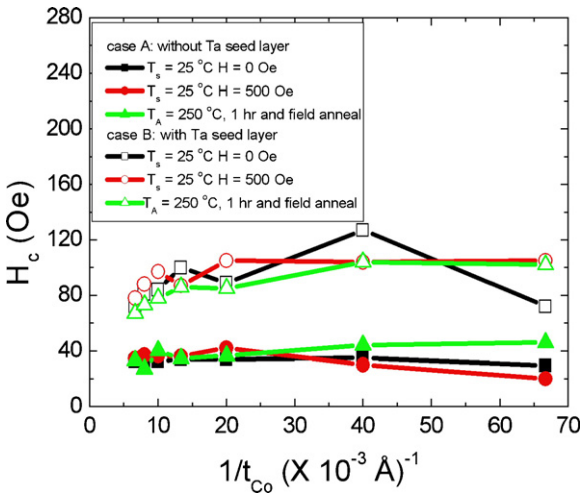

Fig. 5. Coercivity (H_c) versus the inverse of Co thickness ($1/t_{Co}$) in cases A and B, obtained by VSM.

slightly larger than those without a Ta seed-layer are, except for the beginning of two square-data curves. It can be possibly concluded that the random spins arrangement of thinner Co thickness exists in the Ta seed layer, results in lower H_{ex}. Finally, from this figure, the Ta-seeded Co(25 Å)/IrMn(90 Å) sample has the highest H_{ex} value, approximately 205 Oe. Fig. 4(b) plots J_k versus t_{Co}. In the general case, M_s tends to saturate with sufficient increase in t_{Co}. The dependence of J_k on t_{Co}, seen in Fig. 4(b) is similar to the trend in M_s on t_{Co} seen in Fig. 4(a), and similarly, J_k tends to saturate slowly as t_{Co} increases. According to calculation, based on Eq. (1), the J_k has an optimal value of 0.11 erg/cm^2 for the post-annealed Ta-seeded Co(75 Å)/IrMn(90 Å) sample. In addition, the deposited-field Ta-seeded Co(150 Å)/IrMn(90 Å) sample also has an optimal value, since the thicker Co thickness exists a higher saturation magnetization, then J_k is enhanced to larger value.

Fig. 5 plots the dependence of H_c on $1/t_{Co}$, and shows that H_c is inversely proportional to t_{Co}. Because of the surface pinning effect present at both the Ta/Co and Co/IrMn interfaces in the Ta-seeded devices, reduction in Co thickness (t_{Co}), induces an increase in H_c, due to an increased contribution to the pinning effect at the Co/IrMn interface from the Ta/Co interface [21]. The surface pinning effect of Ta/Co and Co/IrMn interfaces possibly exists some defects, including oxide, rough roughness, and inclusions. The defects can induce the displacement of domain walls motion difficulty and the H_c becomes higher values.

4. Conclusion

The variables H_{ex}, J_k and H_c of Ta-seeded and un-seeded Co/IrMn were investigated. Together, post-deposition annealing treatment, and the formation of a Ta seed layer on the Co/IrMn system create the strongest IrMn (1 1 1) texture and the highest value for the exchange-bias field, H_{ex}. Adding a Ta seed layer alone, does not always result in stronger IrMn (1 1 1) texturing, although it can increase H_{ex}. Additionally, H_c values of Ta-seeded Co/IrMn devices are significantly associated with t_{IrMn}, which is explained by coupling and decoupling interactions. The H_c values of Ta-seeded and non-seeded devices in the Co/IrMn system are inversely proportional to t_{Co}, because of surface pinning in the Ta/Co and Co/IrMn interfaces. Finally, the optimal maximum values for H_{ex} and J_k in this investigation are 205 Oe and 0.11 erg/cm^2, which occur for post-annealed Ta-seeded Co(25 Å)/IrMn(90 Å) and Co(75 Å)/IrMn(90 Å) devices, respectively.

Acknowledgments

This work was supported by the National Science Council and I-Shou University, under grants no. NSC97-2112-M214-001-MY3 and ISU98-S-02.

References

[1] T. Hughes, K. O'Grady, H. Laidler, R.W. Chantrell, J. Magn. Magn. Mater. 235 (2001) 329.
[2] Y.T. Chen, Nanoscale Res. Lett. 4 (2009) 90.
[3] I Ken-ichi, M Tsunoda, M Takahashi, Appl. Phys. Lett. 85 (2004) 3812.
[4] K.M. Chui, D. Tripathy, A.O. Adeyeye, J. Appl. Phys. 101 (2007) 09E512.
[5] V.K. Sankaranarayanan, S.M. Yoon, D.Y. Kim, C.O. Kim, C.G. Kim, J. Appl. Phys. 96 (2004) 7428.
[6] J. van Driel, F.R. de Boer, K.-M.H. Lenssen, R. Coehoorn, J. Appl. Phys. 88 (2000) 975.
[7] E. Bailey William, Zhu Nan-Chang, Shan. Robert Sinclair, X. Wang, J. Appl. Phys. 79 (1996) 6393.
[8] D. Lacour, O. Durand, J.-L. Maurice, H. Jaffrès, F. Nguyen Van Dau, F. Petroff, P. Etienne, J. Humbert, A. Vaurès, J. Magn. Magn. Mater. 270 (2004) 403.
[9] Y.T. Chen, S.U. Jen, Y.D. Yao, J.M. Wu, J.H. Liao, T.B. Wu, J. Alloys Compd. 448 (2008) 59.
[10] K. O'Grady, L.E. Fernandez-Outon, G. Vallejo-Fernandez, J. Magn. Magn. Mater. 322 (2010) 833.
[11] N.P. Aley, G. Vallejo-Fernandez, R. Kroeger, B. Lafferty, J. Agnew, Y. Lu, K. O'Grady, IEEE Trans. Magn. 44 (2008) 2820.
[12] G. Anderson, Y. Huai, L. Milowslawsky, J. Appl. Phys. 87 (2000) 6989.
[13] X. Peng, A. Morrone, K. Nikolaev, M. Kief, M. Ostrowski, J. Magn. Magn. Mater. 321 (2009) 2902.
[14] M.A. Seigler, IEEE Trans. Magn. 43 (2007) 651.
[15] D.G. Hwang, S.W. Kim, B.K. Kim, J.Y. Lee, J.K. Kim, J.R. Rhee, S.S. Lee, J. Magn. Magn. Mater. 272–276 (2004) e1417.
[16] G. Malinowski, M. Hehn, S. Robert, O. Lenoble, A. Schuhl, J. Appl. Phys. 98 (2005) 113903.
[17] M. Tafur, W. Alayo, V.P. Nascimento, Y.T. Xing, E. Baggio-Saitovitch, Thin Solid Films 518 (2010) 4312.
[18] V.S. Gornakov, O.A. Tikhomirov, C.G. Lee, J.G. Jung, W.F. Egelhoff Jr., J. Appl. Phys. 105 (2009) 103917.
[19] M. Ali, C.H. Marrows, M. Al-Jawad, B.J. Hickey, A. Misra, U. Nowak, K.D. Usadel, Phys. Rev. B 68 (2003) 214420.
[20] S.N. Piramanayagam, H.B. Zhao, J. Magn. Magn. Mater. 312 (2007) 476.
[21] S.U. Jen, Y.D. Yao, Y.T. Chen, J.M. Wu, C.C. Lee, T.L. Tsai, Y.C. Chang, J. Appl. Phys. 99 (2006) 053701.